Published by
NIGERIAN SOCIETY OF PHYSICAL SCIENCES
Available online @ https://asr.nsps.org.ng/index.php/asr

African Scientific Reports 1 (2022) 23–31

African Scientific Reports

Mechanical Characterization of Armchair and Zigzag Single-walled Carbon Nanotube

R. Hamood[a], Samia Jamal[a], Zina A. Al Shadidi[b,*]

[a]*Department of Physics, Faculty of Education/Saber, University of Aden, Yemen*
[b]*Department of Physics, Faculty of Education/Aden, University of Aden, Yemen*

Abstract

The stress-strain and Young's modulus values of single-walled carbon nanotubes SWCNTs are modeled through linear finite element simulations and Matlab codes, in this study. Cylindrical zigzag and armchair single-walled are established as carbon nanostructures. An individual carbon nanotube (CNT) is simulated as a frame-like structure and the primary bonds between two nearest-neighboring carbon atoms are treated as 3D beam elements. The stiffness and the stress-strain curved of the SWCNTs are investigated. The effect domination of the nanotube diameter of the CNTs on Young's modulus is studied. The simulation results acquired in this study are in good agreement with the experimental results.

DOI:10.46481/asr.2022.1.1.19

Keywords: Single walled Carbon nanotubes, Mechanical properties, Finite element analysis, Young's modulus

Article History :
Received: 14 February 2022
Received in revised form: 01 April 2022
Accepted for publication: 02 April 2022
Published: 29 April 2022

© 2022 The Author(s). Published by the Nigerian Society of Physical Sciences under the terms of the Creative Commons Attribution 4.0 International license. Further distribution of this work must maintain attribution to the author(s) and the published article's title, journal citation, and DOI.

Communicated by: Wasiu Yahya

1. Introduction

Carbon nanotubes (CNTs) are devices in which carbon properties are inherent [1]. The CNTs contains only sp [2] hybridized carbon atoms in a cylindrical structure, these are including the CNTs single-walled carbon nanotubes (SWCNTs) and multi-walled carbon nanotubes (MWCNTs) [2]. The SWCNTs diameters are 0.4-3 *nm*, and 2-500 *nm* for MWCNTs. depending at the technique of synthesis [3]. Carbon nanotubes used as additives to many structural materials, and later as an autonomous device for electronics, optics, plastics, and other materials of nanotechnology fields [4]. CNTs present numerous remarkable properties which include high tremendous strength, aspect-ratio, and

*Corresponding author tel. no:
Email address: zabaqer@yahoo.com (Zina A. Al Shadidi)

high thermal conductivity, ultra-lightweight. The significant electronic properties of CNTs starting from metallic to semiconducting [5]. Their impressive structural, electronic, and mechanical properties are owing to their small size and mass [6]. There is a strong contradiction between experimental results in literatures. Because of the complexity of characterizing materials at the atomic scale and the difficulty of the transition in measurements from micro to macro to elect the results from them. Researchers in experimental studies agreed on nanotubes unparalleled mechanical properties. While we found that the results of practical experiments are scattered and not identical. According to this point of view, simulations used to extract the mechanical properties for the nanotubes, is more accurate method [7].

Finite element method FEM, molecular dynamics, continuum mechanics, and experimental measurements are the most usable methods in calculating the properties of nanostructures [8].

This paper evaluated the single-wall nanotubes with different diameters. The nanostructures were modeled using the finite element method approach by beam elements. The carbon atoms were taken into consideration to be finite elements nodes. Zigzag and armchair-type cylindrical tubes have been acquired by computer programming techniques together with the finite element analysis (FEM).

2. Computational Methodology

There are many ways to view a SWCNT. Carbon cell has a hexagonal shape repeated periodically each carbon atom attached to the tree other atoms by the strong covalent bond. As a results of the strong bonds and ideal engineering links, nanotubes and all nano structures have a strong mechanical characteristic [9]. The chiral vector and the chiral angle determine mechanical properties [10]. The above description was done by using MATLAB code to plot the carbon Sheet after rolling it to calculate in an accurate computational manner the atomic and bonds sites, according to the (n, m) values. These sites will be written in Excel files as nodes and elements respectively.

The second step will be the way to calculate strain resulting from the stress on one of the tube ends. The stress will result in changing the angle between bonds in a way that the following equations control the deformation that happened in the tube due to the applied stress.

The chiral vector and angle defined in terms of the lattice translation indices (n, m); i.e. the basic vectors $\vec{a}_1$ and $\vec{a}_2$ and the hexagonal lattice is described as [11]:

$$\vec{C}_h = n \cdot \vec{a}_1 + m \cdot \vec{a}_2, \tag{1}$$

$$L = \left|\vec{C}_h\right| = a \cdot \sqrt{n^2 + nm + m^2}, \tag{2}$$

$$\theta = sin^{-1}\left[\frac{\sqrt{3}m}{2\left(\sqrt{n^2 + nm + m^2}\right)}\right]. \tag{3}$$

Our model based on the elastic properties of single-walled carbon nanotubes; the model used finite element method to simulate the covalent bonds. The structural properties of chemical bonds can be determined through energies of stretching, bending, and torsion, which is based on Odegard's methodology [11]. A hypothetical regular bond has a definite strain energy, as a result of the tensile bending and torsion energy will be represented [12] as follows:

$$U_A = \frac{1}{2}\int_0^L \frac{N^2}{EA}dl = \frac{1}{2}\frac{N^2 L}{EA} = \frac{1}{2}\frac{EA}{L}(\Delta L)^2, \tag{4}$$

$$U_M = \frac{1}{2}\int_0^L \frac{M}{El}dl = \frac{1}{2}\frac{2El}{L}\alpha^2 = \frac{1}{2}\frac{El}{L}(\Delta\alpha)^2, \tag{5}$$

$$U_T = \frac{1}{2}\int_0^L \frac{T^2}{GJ}dl = \frac{1}{2}\frac{T^2 L}{GJ} = \frac{1}{2}\frac{GJ}{L}(\Delta\beta)^2. \tag{6}$$

U_A, U_M, and U_T are the axial strain energy, the bending energy, and the torsion energy, respectively. L is the length, A represents the cross section area, I is the moment of inertia, J is the polar moment of inertia for the beam cross section,

E Young's modulus, G represents shear modulus of the beam. Another MATLAB code to be written, to calculate the stiffness matrix for each bond, then the stiffness matrix for the nanotube and plot stress-strain curves, beginning from the nodes and elements files resulting from the first MATLAB code. The specified information for our code is the tube length, tube diameter, EA, EI, and GJ. The code performed to calculate the strain in each tube due to a subjected force on one end of the nanotube. The mathematical approach used in those calculations will be defined as follows. The structure beam stiffness will be related in term of the force field constants as follows [12]

$$\frac{EA}{L} = k_r, \tag{7}$$

$$\frac{El}{L} = k_\theta, \tag{8}$$

$$\frac{GJ}{L} = k_\phi. \tag{9}$$

The total strain and stress are respectively calculated using the following equations [13]:

$$\epsilon = \frac{\Delta L}{L_o}, \tag{10}$$

$$\sigma = \frac{F}{A}, \tag{11}$$

where $\Delta L = (L - L_o)$, L is the current length, L_o is the initial length, F is the applied tensile force which is calculated by totaling the whole number of the reaction forces at the fixed nodes and A is the cross section area of the CNT, which is defined as $A = \pi Dt$ (where $D = CNT$ diameter and t is the thickness of a single-wall carbon nanotube is taken as 3.4 Å). The slope of the stress-strain curve in this range gives Young's modulus (Y)

$$Y = \frac{\sigma}{\epsilon} = \frac{F/A}{\Delta L/L_o}, \tag{12}$$

where is the ratio of normal stress (σ), (ϵ) represents the normal strain from a uni-axial tension test, while (Y) is the Young's modulus [14].

3. Result and Discussion

3.1. Structural Characteristics of Carbon Nanotubes

To verify the reliability and efficiency of the structural mechanic's approach to the modeling of carbon nanotubes and to illustrate its capability, we design graphite sheets as single-walled carbon nanotubes as shown in Figure 1, then roll it to perform a (SWCNTs), and to calculate a number of their basic elastic properties, such as stress-strain, stiffness and Young's modulus.

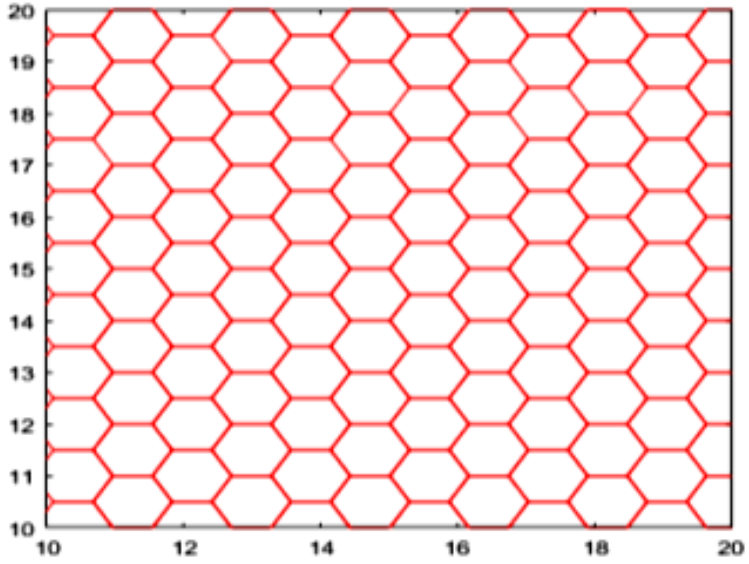

Figure 1. CNTs as a hexagonal graphene sheet.

As a result of the first computational step with the first MATLAB code, the CNTs' shapes were plotted, and the locations of the (atoms) nodes and (bonds) elements were calculated as it should be. The geometrical parameters for zigzag and armchair nanotubes were obtained according to the default chirality (n, m) values. Four armchair models, there chirality was (12, 12), (17, 17), (22, 22), (30, 30), and three zigzag models (12, 0), (22, 0), (30, 0).

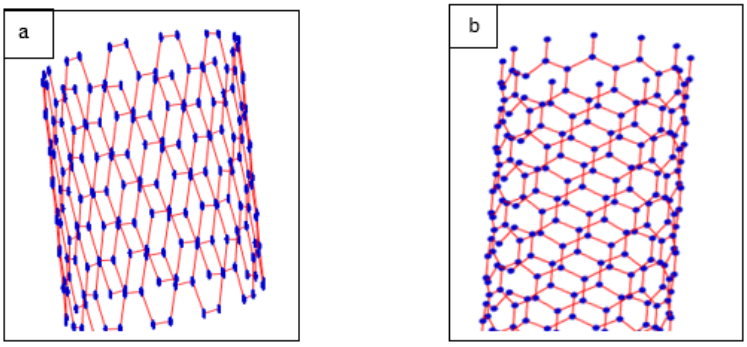

Figure 2. Graphene sheet that forms (a) an armchair and (b) zigzag SWCNT when rolled parallel to x-axis.

The two CNTs with armchair chirality (12, 12) and zigzag chirality (12, 0) shown in (Fig. 2a,b) are modeled and analyzed. The bond length for both types is 2.3382 *nm* and the length of the graphene sheets is 20 *nm*.

3.2. Mechanical Characteristics of Carbon Nanotubes

In the first parametric study for a single wall armchair SWCNTs, and a single wall zigzag CNTs. Three stiffness parameters need to be decided. They are EA, EI and GJ can be transformed into force constants. These force constants are known, as the $C-C$ bond. The cross-section for each nanotube is assumed to be circular with diameter calculated in the first MATLAB code for every nanotube, and used in this search stage. Force constants used in this step become as follows: $EA = 6.52\times10^{-7}\ N/nm$, $EI = 8.76\times10^{-10}\ N\cdot nm/rad^2$ and $GJ = 2.78\times10^{-10}\ N\cdot nm/rad^2$. After calculating the stiffness matrix of the bond, the stiffness matrix for the tube was calculated. The $C-C$ bonds were represented with the elastic beam mesh elements.

The reason for considering the planar frame normal to the cylinder base is the reduction of the unknown displacements for the structure system, and putting the whole displacements in a matrix. In the finite element method, displacements for the joint components required are a translation in the Z direction and rotations about the X and Y axes. The z-axis in local coordinates and the z-axis in global coordinates will coincide; therefore, linear displacement along the z-axis will be identical, while the x and y-axes required accurate calculations for transformation to the global axis because of the rotational and translational components of nodal coordinates.

Notice the existence of three kinds of stiffness sources at each node as shown in Equations (4, 5, & 6). Therefore, before assembling the corresponding matrices for the nanotube structure, the references of these matrices must be transformed to the global system of coordinates. And because of conceding the Z-axis of the local coordinates with the Z-axis for the global system, the rotation will be happened in the x-y plane. The corresponding matrices will be calculating through the relationship between moment components at each node and for the three axes [15].

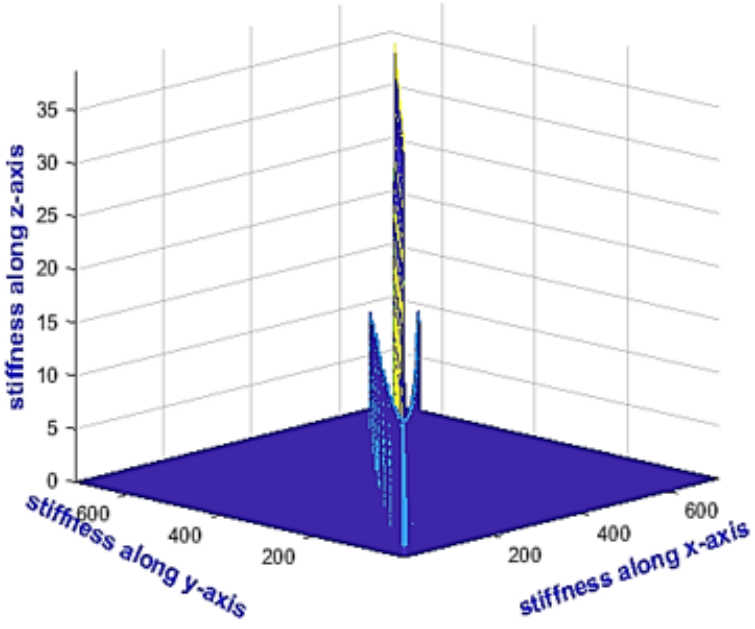

Figure 3. Stiffness matrix for (12, 12) nanotube, the clearest view from polar angle rotation.

In concerning to the stiffness matrices, Figure 3 above shows the stiffness matrix for a $Az : -46$, $EL = 15$ view in Matlab figure plot. This figure obvious that the stiffness directions in the nodes matrix. All the stiffness planes represent the planes gathering of strengths points in the nanotube. The highest plane is along the $k_z - axis$, this plane refers to the highest resistance to deformation or fracture when shed a deformation force along $k_z - axis$. In the current study, the nanotube length supposed to be along the z-axis, where the nanotube base lies on the x-y plane. The x and y axis length plotted according to the nanotube diameter. According to the above description, the reader could imagine a standing nanotube along the z- axis.

The above stiffness plane tells that cutting the carbon nanotube into two similar shells is impossible. In the same figure there are two planes starting from the same vector there are two stiffness planes starting from the same $k_z - vector$ starting from the (0, 0) point and rising up to 12.93, and making a 30 *degree* angle with the first stiffness plane. These two planes refer to other strong places in the nanotubes structure. These two planes starting from the same line the line height is 29.39 *nm* and slanted from the main plane by an angle equal to 30 *degrees*, this angle formed according to the rotation angle of the bonds or joints along the x-axis and y-axis.

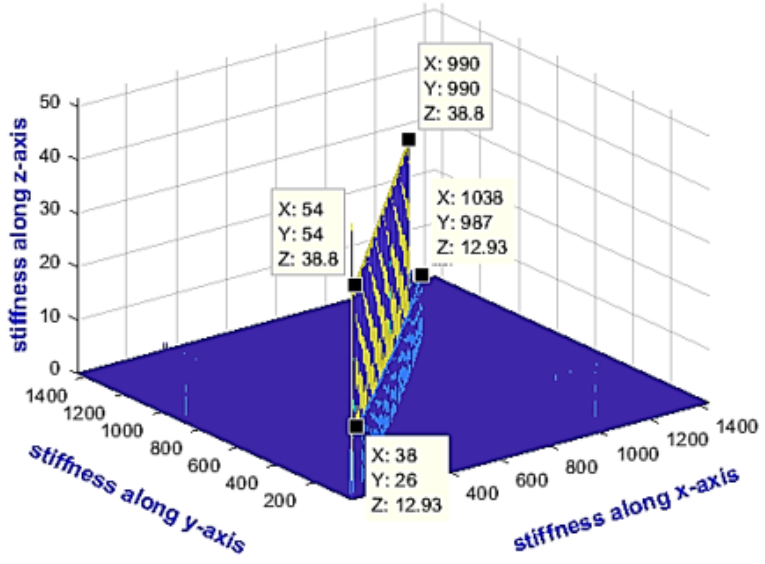

Figure 4. The stiffness matrix for armchair (12, 12).

In Figure 4, it is obvious that the maximum point on the middle plane is (990, 990, 38.8). The strength points reach to a high level while it is less in the side planes and equal to (1038, 987, 12.93). The stiffness due to elongation due to the applied force in the nanotube is clear in the z-value at the middle plane (38.8). In the two other planes, the x-axis reaches to 1038 *units*. In all the stiffness planes x maximum point and y- maximum point is much higher than the z- maximum point due to the rotation action on the atomic bonding along these two axes.

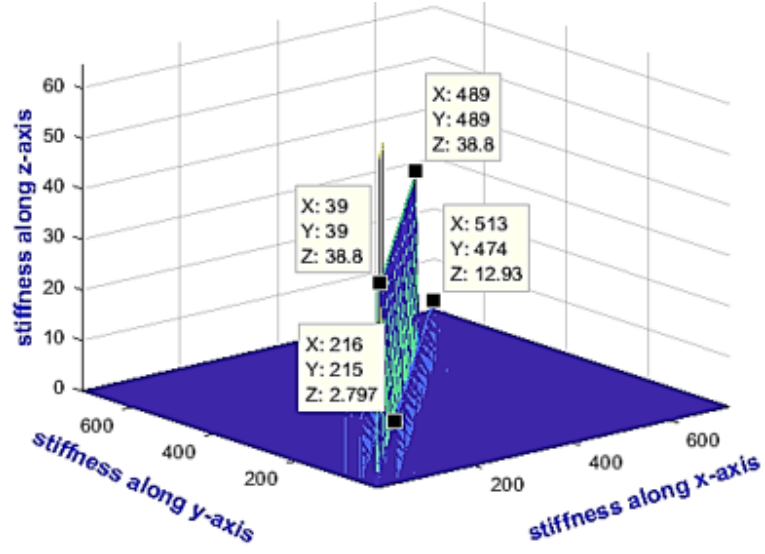

Figure 5. The stiffness planes for Zigzag (12, 0).

Figure 5 shows the maximum point is (489, 489, 38.8) and the lower plane reach (513, 474, 12.93). The strength planes in the two kinds of nanotubes shows an equal maximum point at z-axis (height), and lower length and width in the zigzag type. The lower x-axis and y-axis values mean lower strength and more fracture ability.

From the stiffness matrix and a more force subjected on one of the nanotubes ends the stress-strain relation for each nanotube, was calculated and plotted in Figure 6.

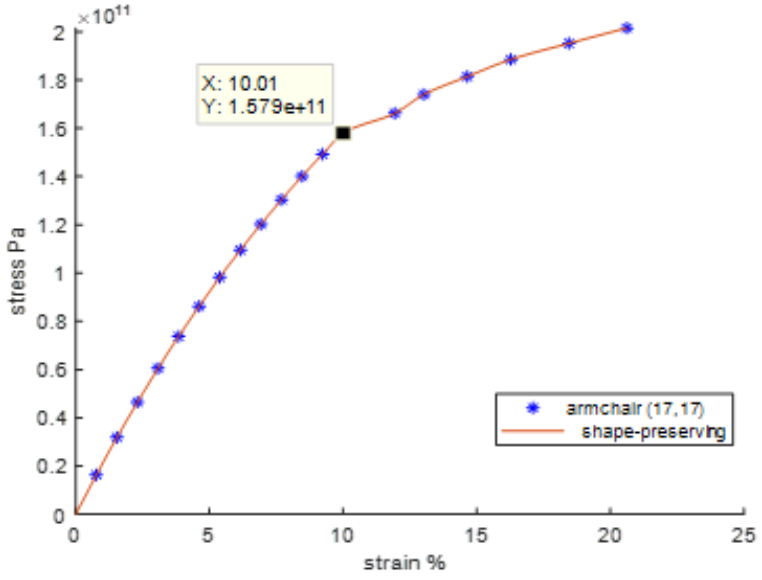

Figure 6. The stress-strain relation in armchair nanotube with shape preserving fitting.

Figure 6 shows the stress-strain relation for single wall armchair (17, 17) carbon nanotube. Two regions are clear the first region is linearly dependent, and the second region where the stress changed its behavior after the (0.1579 GPa). To determine the mathematical approach is finite element method (FEM), enable to show the elastic mechanical behavior of the SWCNTs.

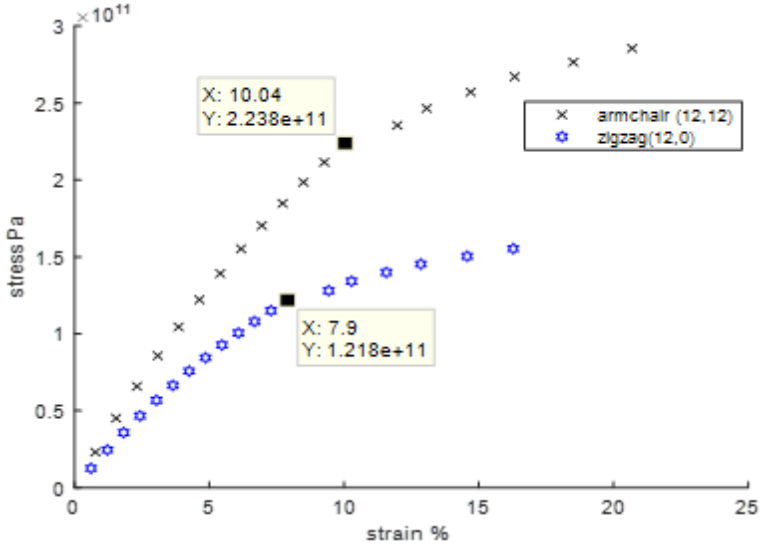

Figure 7. Stress-strain comparison curves of armchair and zigzag SWCNTs.

The variation of stress-strain curves of armchair (12, 12) chirality and zigzag (12, 0) chirality SWCNTs is shown in Figure 7. It is clear that: the stress–strain values increase linearly up to an inflection point (peak force) occurs at about 10.04 % strain for an armchair and 7.9 % strain for zigzag, and then increases gradually with non-linearity at large stress-strain values. The stress- strain of the armchair and zigzag SWCNTs are 0.223 TPa and 0.1214 TPa, respectively. Based on the curves, the stress-strain value of armchair is larger than that of zigzag. This may be due

to the existence of bonds between unstable edge atoms in the armchair, which is not present in zigzag SWCNTs [16]. The calculated results are in the equal order as the ones suggested within the literature [17].

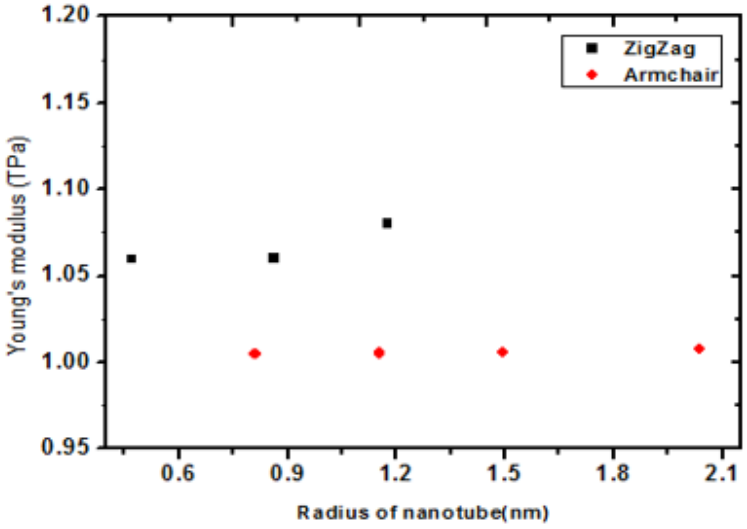

Figure 8. Young's modulus for armchair and zigzag SWCNTs with various CNT diameter using Morseforce.

The calculated Young's modulus is plotted against the nanotube diameter for armchair and zigzag SWNTs using More force method, in Figure 8. It could be seen that the trend is similar for both armchair and zigzag SWNTs; Young's modulus increased slightly. In general young's modulus increased with the diameter. This could be attributed to the effect gradually diminishes of curvature with the CNT diameter increase [18]. FE simulation results for Young's modulus and nanotube diameters are listed in Table 1. Those values are in good agreement with the theoretical results of Lu & Huang [17] and experimental results of Chuo & Li [19].

Table 1. Finite element simulation results of young's modulus and diameters values of Armchair & Zigzag SWNTs.

Model/Chirality (n, m)	**Diameter** (*nm*)	**Young's Modulus** (*TPa*)
Armchair (12,12)	0.814	1.0046
Armchair (17,17)	1.1534	1.0055
Armchair (22,22)	1.4927	1.0056
Armchair (30,30)	2.0354	1.0077
Zigzag (12,0)	0.470	1.0599
Zigzag (22,0)	0.8617	1.06
Zigzag (30,0)	1.1752	1.08

4. Conclusion

Within this computational study, a structural mechanics approach has been developed for modeling single-wall carbon nanotubes via finite element method (FEM), two graphene sheets with armchair chirality (12,12) and zigzag chirality (12,0) are modeled and analyzed for the comparison between the armchair and zigzag type based on the chirality. The values of stress-strain and young's modulus of SWCNTs are acquired. The stress–strain values increase linearly before reaching the force peak. An inflection point (force peak) take place at about 10.4 % strain for an armchair and 7.9 % strain for zigzag, and then increase gradually. Young's modulus E increases with increasing nanotube diameter. The tube deformation decreased with increasing the diameter of the tube.

Acknowledgments

We thank the referees for the positive enlightening comments and suggestions, which have greatly helped us in making improvements to this paper.

References

[1] P. M. Alderton, J. Gross & M. D. Green, "Comparative study of doxorubicin, mitoxantrone, and epirubicin in combination with ICRF-187 (ADR-529) in a chronic cardiotoxicity animal model", Cancer Res. **52** (1992) 194. http://aacrjournals.org/cancerres/article-pdf/52/1/194/2446804/cr0520010194

[2] D. Tasis, N. Tagmatarchis, A. Bianco & M. Prato, "Chemistry of carbon nanotubes", Chem. Rev. **1063** (2006) 1105. https://pubs.acs.org/doi/10.1021/cr050569o

[3] S. N. Kim, J. F. Rusling & F. Papadimitrakopoulos, "Carbon nanotubes for electronic and electrochemical detection of biomolecules", Adv. Mater. **19** (2007) 3214. https://doi.org/10.1002/adma.200700665

[4] Y. Zhang, Y. Bai & B. Yan, "Functionalized carbon nanotubes for potential medicinal applications", Drug discovery today **15** (2010) 428. https://doi.org/10.1016/j.drudis.2010.04.005

[5] L. Luer, S. Hoseinkhani, D. Polli, J. Crochet, J. Hertel & G. Lanzani, "Size and mobility of excitons (6,5) carbon nanotubes", Nat. Phys. **5** (2009) 54. https://doi.org/10.1038/nphys1149

[6] Y. Usui, H. Haniu, S. Tsuruoka & N. Saito, "Carbon nanotubes innovate on medical technology", Medicinal Chemistry **2** (2012) 1. https://doi.org/10.4172/2161-0444.1000105

[7] R. Rafiee & R. M. Moghadam, "On the modelng of carbon nanotubes: a critical review", Compos. Part B **56** (2014) 435. https://doi.org/10.1016/j.compositesb.2013.08.037

[8] J. L. Tsai & J. F. Tu, "Characterizing mechanical properties of graphite using molecular dynamics simulation", Materials & Design **31** (2010) 194. http://dx.doi.org/10.1016/j.matdes.2009.06.032

[9] K. Lau, C. Gu & D. Hui, "A critical review on nanotube, /nanoclay related polymer composite materials", Compos. Part B Eng. **37** (2006) 425. https://doi.org/10.1016/j.compositesb.2006.02.020

[10] E. T. Thostensona, Z. Renb & T. W. Choua, "Advances in the science and technology of carbon nanotubes and their composites a review", Compos. Sci. Technol. **61** (2001) 1899. https://doi.org/10.1016/S0266-3538(01)00094-X

[11] G. M. Odegarda, T. S. Gates, L. M. Nicholsonc & K. E. Wise, "Equivalent –continuum modeling of nano-structured materials", Composites Sci. and Techno. **62** (2002) 1869. https://doi.org/10.1016/S0266-3538(02)00113-6

[12] N. Khandoker, S. Islam & Y. S. Hiung, "Finite element simulation of mechanical properties of graphene sheets", IOP Conf. Series: Materials Science and Engineering **206** (2017) 012057. https://doi.org/10.1088/1757-899X/206/1/012057

[13] C. Baykasoglul & A. Mugan, "Failure analysis of graphene sheets with multiple stone-thrower-wales defects using molecular-mechanics based nonlinear finite element models", Hittite Journal of Science and Engineering **5** (2018) 19. https://doi.org/10.17350/HJSE19030000073

[14] X. L. Li & J. G. Guo, "Theoretical Investigation on failure strength and fracture toughness of precracked single-Layer graphene sheets", Hindawi Journal of Nanomaterials (2019) 1. https://doi.org/10.1155/2019/9734807

[15] P. Papanikos, D. D. Nikolopoulos & K. I. Tserpes, "Equivalent beams for carbon nanotubes", Comput Mater Sci **43** (2008) 345. https://doi.org/10.1016/j.commatsci.2007.12.010

[16] Q. Lu, W. Gao & R. Huang, "Atomistic simulation and continuum modeling of graphene nanoribbons under uniaxial tension", Modelling and Simul. Mater. Sci. Eng. **19** (2011) 1. https://doi.org/10.1088/0965-0393/19/5/054006

[17] Q. Lu & R. Huang, "Excess energy and deformation along free edges of graphene nanoribbons", Phys. Rev. B **81** (2010) 1. https://doi.org/10.1103/PhysRevB.81.155410

[18] E. G*ü*nay, "Modelling of single walled carbon nanotube cylindrical structures with finite element method simulations", AIP Conference Proceedings **1727** (2016) 020009-1. https://doi.org/10.1063/1.4945964

[19] T. W. Chou & C. A. Li, "Structural mechanics approach for the analysis of carbon Nanotubes", Int. J. Solids Struct. **40** (2003) 2487. https://doi.org/10.1007/s11012-009-9222-2